Structural Chemistry
https://doi.org/10.1007/s11224-020-01529-5

ORIGINAL RESEARCH

Synthesis, characterization, and hypoglycemic efficacy of nitro and amino acridines and 4-phenylquinoline on starch hydrolyzing compounds: an in silico and in vitro study

Lohitha Narayanaswamy[1] · Suresh Yarrappagaari[2] · Srinivasulu Cheemanapallia[3] · Rajeswara Reddy Saddala[2] · V. Vijayakumar[1]

Received: 17 October 2019 / Accepted: 30 March 2020

Abstract

α-Amylase and α-Glucosidase are important therapeutic targets for type II diabetes. The present focus of our study is to elucidate the hypoglycemic activity of novel compounds through in vitro and in silico studies. Here, we synthesized the nitro acridines (**3a–3c),** amino acridines **(4a–4c**), and nitro phenylquinoline (**3d)** and amino phenylquinoline **(4d**) using a multi-step reaction protocol in good yields. All the above derivatives were screened for molecular docking, α-Amylase and α-Glucosidase inhibitory activities utilizing acarbose as standard drug. In silico studies were performed to explore the binding ability of compounds with the active site of α-Amylase and α-Glucosidase enzymes. The in vitro antihyperglycemic report of **3c** exhibits the maximum inhibitory activity with IC_{50} values of 200.61 ± 9.71 μmol/mL and 197.76 ± 8.22 μmol/mL against α-Amylase and α-Glucosidase, respectively. Similarly, the compound **3a** exhibits IC_{50} values of 243.78 ± 13.25 μmol/mL and 296.57 ± 10.66 μmol/mL, and **4c** exhibits IC_{50} values of 304.28 ± 3.51 μmol/mL and 278.86 ± 3.24 μmol/mL with a significant $p < 0.05$ in both enzyme inhibitions. In addition, the presence of diverse functional moieties in synthesized compounds may provide a strong inhibitory action against the abovementioned enzymes compared with standard acarbose inhibition (IC_{50}, 58.74 ± 3.68 μmol/mL and 49.39 ± 4.94 μmol/mL). Also, the docking studies provided an excellent support for our in vitro studies. The outcome of these studies recommends that the tested compounds might be treated as potential inhibitors for the starch hydrolyzing enzymes in type II diabetes.

Keywords Nitro and amino acridines · Nitro and amino 4-phenylquinoline · Antihyperglycemic activity · α-Amylase · α-Glucosidase · Docking

Introduction

Diabetes mellitus is the largely widespread universal endocrine disease, and its commonness is mounting at a disturbing pace currently affecting 3% of the world population [1]. This complex metabolic disease is the most important human health distress in the world, and it may approximately influence 300 million people by the year 2025 [2]. This progressive metabolic disorder is characterized by the constant increase of blood glucose level which finally leads to macro-vascular (brain stroke, heart disease, hypertension, peripheral arterial disease, and foot problems) and microvascular (retinopathy, cataracts, renal failure, blood vessels, and neuropathy) damages in several tissues [3]. This results in blood sugar levels, a circumstance characteristically called diabetes. The body required insulin to convert sugar, starch, and other food into energy. The symptoms of this disorder are polydipsia, polyphagia, polyuria, weight loss, etc.

Mammalian pancreatic α-Amylase inhibitors propose an efficient approach to lessen the levels of postprandial high

Electronic supplementary material The online version of this article (https://doi.org/10.1007/s11224-020-01529-5) contains supplementary material, which is available to authorized users.

✉ V. Vijayakumar
kvpsvijayakumar@gmail.com

[1] Centre for Organic and Medicinal Chemistry, VIT University, Vellore, Tamil Nadu 632014, India

[2] Department of Biotechnology, Division of Animal Biotechnology, Dravidian University, Kuppam, Andhra Pradesh 517426, India

[3] Department of Biochemistry, Sri Krishnadevaraya University, Anantapuramu, Andhra Pradesh 515003, India

Published online: 15 June 2020

blood glucose levels through control of starch breakdown. Pancreatic α-Amylase is responsible for the hydrolysis of starch to a combination of minor oligosaccharides consisting of maltose, maltotriose, and a quantity of α-(l-6) and α-(1-4) oligoglucans [4]. Inhibitors of α-Amylase and α-Glucosidase postpone the breaking of carbohydrate in the small intestine and diminish the postprandial blood glucose digression levels in diabetic patients [5]. Hence, the inhibition of α-Glucosidase and α-Amylase prominent enzymes has been established as a functional and efficient strategy to lessen the levels of postprandial hyperglycemia.

Several antidiabetic commercial drugs such as acarbose, voglibose, and miglitol are currently available in the market in use for the treatment of α-Amylase and α-Glucosidase enzyme inhibition in diabetes mellitus [6]. No single prescription is obtainable as a comprehensive solution to this. However, these drugs are not wished to be worn constantly for a long time, due to their rigorous side effects [7]. Therefore, the researchers are focused to develop the safer, single, and more tolerable α-Glucosidase inhibitors with lesser side effects for the treatment of the diabetic disorder. To evaluate the antidiabetic activity of synthetic compounds, in vitro and in vivo methods are adopted [8].

The design of gracious chemical units like acridine and quinoline derivatives could lead to the development of new drugs for the treatment of various diseases. Acridine derivatives are known for their various chemical and biological activities [9]. It is also broadly accounted that acridine, an *N*-donor ligand, has an affinity to metal complexes, in particular, those of important metals such as Pt and Pd [10, 11]. Due to their different structural and remedial actions, thousands of natural or synthetic acridines have been isolated or developed [12, 13]. The biological activities of acridine can mostly depend on its benzene ring as well as on $–NHCH_2CH_2-$ or $–NHCH_2-$ part [14]. Acridine core was reported to have antioxidant, antibacterial, anticancer, antimalarial, and mutagenic properties, mostly associated with their ability to inhibit the enzymes acting on nucleic acids [15]. Moreover, the derivatization of acridine was demonstrated to improve the biological effectiveness of acridine and reduce its side effects subsequently interaction with DNA [16]. Hence, the synthesis of new derivatives of acridines is a fascinating field for researchers in their quest to discover novel potent antidiabetic drugs.

Computer-assisted drug innovation reached significance mostly because of the dependability in the results and overlays a new technique for the research hub toward the substitute animal models. Molecular docking serves this purpose [17]. Protein-ligand relations are equivalent to the lock-and-key code, in which the lock encodes the protein and the key is a cluster with the ligand. The major dynamic forces for binding materialize to be hydrophobic interaction [18]. Hence, the investigation of compounds with reasonable α-Amylase enzyme inhibitory property and α-Glucosidase enzyme inhibition is necessary for the new drug development. In this study, the objective was to synthesize novel nitro and amino acridines 7-nitro-9-phenyl-3, 4-dihydroacridine-1(2*H*)-one (**3a**), 7-amino-9-phenyl-3, 4-dihydroacridine-1(2*H*)-one (**4a**), 3, 3-dimethyl-7-nitro-9-phenyl-3, 4-dihydroacridine-1(2*H*)-one (**3b**), 7-amino-3, 3-dimethyl-9-phenyl-3, 4-dihydroacridine-1(2*H*)-one (**4b**), 5,6,7,8-tetrahydro-2-nitro-9-phenylacridine (**3c**), 9-phenyl-5, 6, 7, 8-tetrahydroacridine-2-amine (**4c**), and nitro phenylquinolines (Ethyl 2-methyl-6-nitro-4-phenylquinoline-3-carboxylate (**3d**) and Ethyl 6-amino-2-methyl-4-phenylquinoline-3-carboxylate (**4d**) derivatives) and to evaluate their inhibitory activity against both α-Amylase and α-Glucosidase with reference to in silico studies. The findings of the work may lead to develop novel α-Glucosidase inhibitors with higher potential and reduced risk of secondary complications which are in general associated with type2 diabetes mellitus.

Results and discussion

Chemistry

Synthesis and characterization of acridine- and phenylquinolines-based derivatives

Initially, the compound **1** was converted to nitro acridines and nitro phenylquinolines **3a–d** according to Scheme 1. The nitro group of the obtained compounds **3a–d** was reduced into a corresponding primary amino group using NH_4Cl/Zn dust in dioxane/water (1:1). The newly synthesized compounds **3a–c**, **4a–c, 3d**, and **4d** were characterized by one- and two-dimensional NMR and HRMS spectral data (included in the "Experimental" section).

Spectral characterization of compound 4a

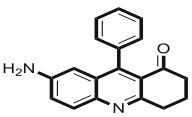

The melting point and ^1H and ^{13}C NMR spectral data of compounds **3a** is found to be in concurrence with literature. The formation of compound **3a**, with the nitro function, was also inferred based on the absorption peak at 3419 cm^{-1} and 3348 cm^{-1} in the IR spectrum, whose disappearance confirmed the conversion of **3a** into **4a**, which is further characterized by ^1H NMR, ^{13}C NMR, H, H-COSY, HSQC, and HRMS (ESI) spectral analysis. The ^1H NMR spectrum of compound 7-amino-9-phenyl-3, 4-dihydroacridine-1(2*H*)-one (**4a**) exhibited the following chemical shifts in the aromatic region: δ ppm 7.87 (d, $J = 9.2$ Hz, 1H), 7.46 (m, 3H), 7.20 (dd, $J = 9.2, 2.4$ Hz, 1H), 7.15 (d, $J = 7.6$ Hz, 2H), and 6.47 (d, $J = 2.4$ Hz, 1H). The careful examination of the above signals

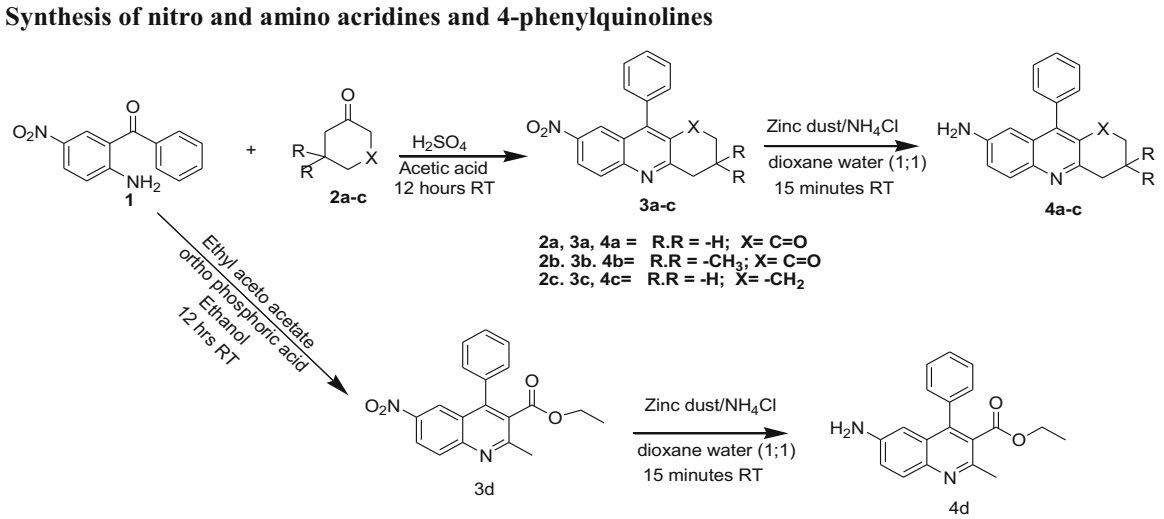

Scheme 1 Synthesis of nitro and amino acridines and 4-phenylquinolines

clearly illustrated that the signals at δ 7.46 (m, 3H) and 7.15 (d, $J = 7.6$ Hz, 2H) are due to the phenyl substituent at C-9. The signal at δ 7.87 (d, $J = 9.2$ Hz, 1H) is due to the proton at C-5. The proton at C-6 has two coupling partners at C-5 and C-8 and hence appeared as a doublet of doublet at δ 7.20 ppm (dd, $J = 9.2$, 2.4 Hz, 1H), and hence, the signal at δ 6.47 ppm (d, $J = 2.4$ Hz, 1H) is assigned to the proton at C-8. The aliphatic region exhibited the following signals at δ 3.85 (s, 2H), 3.30 (t, $J = 6.2$ Hz, 2H), 2.66 (t, $J = 6.4$ Hz, 2H), and 2.24–2.17 (m, 2H). The singlet at δ 3.55 ppm is assigned to two protons of amino function at C-7, and hence, other signals are assigned to protons at C-2, C-3, and C-4 carbons. The ^{13}C NMR spectrum exhibited the following signals: δ 197.4, 157.4, 147.8, 143.5, 143.0, 137.3, 128.6, 127.9, 127.1, 127.0, 126.2, 122.9, 122.8, 106.5, 39.7, 33.2, and 20.5 ppm; the extreme down-field signal at δ 197.4 ppm was assigned to the carbonyl carbon at C-1. The three signals appeared at δ 39.7, 33.2, and 20.5 ppm are due to the methylene carbons at C-2, C-3, and C-4 which was confirmed by DEPT-135 spectrum also; the relatively down-field signal at δ 39.7 ppm was assigned to carbon at C-2 since it may be due to the anisotropy of the neighboring carbonyl group. The signals at δ 33.2 and 20.5 ppm were assigned to carbons C-4 and C-2, respectively. All other signals are due to the aryl carbons of phenyl substituent at C-9 and carbons at the acridine ring. All these spectral data confirmed the formation of the desired molecule. It also further confirmed by the observation of m/z at 288.1260 in the mass spectrum (HRMS-ESI (m/z) calculated for $C_{19}H_{16}N_2O$ $[M]^+$= 288.1263, found = 288.1260). The chemical shift values of the remaining compounds of the series also assigned in a similar fashion and are included in the Methodology section. All the newly synthesized molecules **4a–d** were subjected to in vitro antidiabetic evaluations along with **3a–d** since those molecules also are not yet subjected to these studies; the results are discussed in the "Biology" section.

Biology

In vitro antidiabetic activity of acridine and phenylquinoline based derivatives

In vitro α-Amylase inhibition study Selectivity of α-Glucosidase and α-Amylase inhibitors is of enormous significance, for the reason that unclear inhibition restraint of other glycosidases, transcendently, pancreatic α-Amylase, may the reason for the increments of non-processed sugars in the gut, which in turn results in stomach torment, looseness of the bowels, and farts [19]. The outcomes in both inhibition and IC_{50} values of **3a-c** and **4a-c**, **3d**, **4d**, and acarbose against α-Amylase was represented in Fig. 1a and Table 1 respectively. These results confirmed a considerable dose-depended diminution in α-Amylase enzyme activity. The most significant ($p < 0.05$) inhibition appears in the **3c** (IC_{50} 200.61 ± 9.71 μmol/mL) and **3a** (IC_{50} 243.78 ± 13.25 μmol/mL), whereas **3b** (IC_{50} 389.93 ± 13.88 μmol/mL) showed less potency. Comparatively to an acarbose reference compound, using IC_{50} value, it is estimated to be 58.74 ± 3.68 μmol/mL for acarbose (Table 1) activity higher for those compounds tested. Compounds **4a-c**, **3d**, and **4d** also showed α-Amylase inhibitory activity (IC_{50}, 366.86 ± 17.29, 332.07 ± 14.87, 304.28 ± 3.51, 302.84 ± 6.42, and 319.60 ± 3.24 μmol/mL) which had a poorer effect than **3c** and **3a** derivatives when compared with the standard drug. However, not any of the synthesized compounds show a significant α-Amylase inhibitory activity, whereas the reference drug indicated 71.96% inhibition at a maximum concentration. These outcomes specify that **3c** and **3a** compounds were more useful against α-Amylase.

In vitro α-Glucosidase inhibition study The synthesized amino and nitro derivatives of acridines (**3a–c** and **4a–c**) and

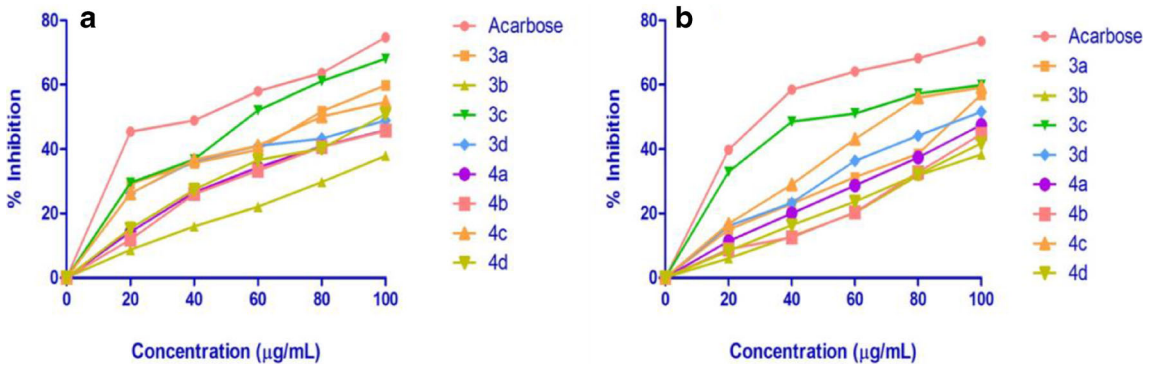

Fig. 1 **a** α-Amylase inhibition and **b** α-Glucosidase inhibition activity in the acridine- and phenylquinoline-based derivatives (**3a-d,** and **4a–d**)

Table 1 In vitro antidiabetic activity of different acridine- and phenylquinoline-based derivatives (**3a-d** and **4a-d**)

Test samples	Compound structure	Molecular weight	α-Amylase inhibition activity IC_{50} values (µmol/mL)	α-Glucosidase inhibition activity IC_{50} values (µmol/mL)
Acarbose	Standard reference	645.60	58.74±3.68[a]	49.39±4.94[a]
3a	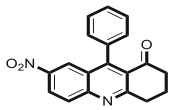	318.10	243.78±13.25[c]	296.57±10.66[d]
3b	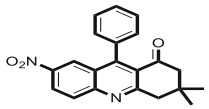	346.38	389.93±13.88[f]	369.33±21.29[f]
3c	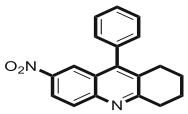	304.34	**200.61±9.71**[b]	**197.76±8.22**[b]
3d	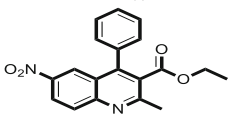	336.34	302.84±6.42[d]	279.94±10.31[c]
4a	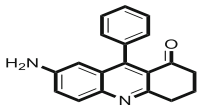	288.13	366.86±17.29[f]	370.92±19.67[e]
4b	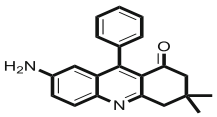	316.40	332.07±14.87[e]	370.73±22.20[e]
4c	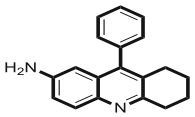	274.36	304.28±3.51[d]	278.86±3.24[c]
4d	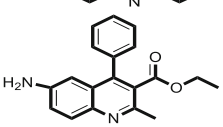	306.36	319.60±3.24[e]	397.76±23.51[g]

Values in the table are represented as mean ± SD for triplicates. Mean ± SD is not allotment a frequent alphabet in the column differ significantly at $p < 0.05$ (performed One Way ANOVA followed by Duncan Post Hoc)

phenylquinolines (**3d** and **4d**) along with acarbose (as reference) were tested for their α-Glucosidase in vitro inhibition action. IC_{50} values and inhibitory activity (%) were given in Table 1 and Fig. 1b. The compound **3c** displayed a significant action against α-Glucosidase (IC_{50} 197.76 ± 8.22 μmol/mL); among the tested compounds, **4c** (IC_{50} 278.86 ± 3.24 μmol/mL) possessed the best inhibition activity which is found to be better than the reference acarbose (IC_{50} 49.39 ± 4.94 μmol/mL). Compounds **3a**, **4a**, **3b**, **4b**, **3d**, and **4d** also showed α-Glucosidase inhibitory activity (IC_{50} 296.57 ± 10.66, 370.92 ± 19.67, 369.33 ± 21.29, 370.73 ± 22.20, 279.94 ± 10.31, and 397.76 ± 23.51 μmol/mL, respectively) but not better than **3c, 4c,** and acarbose. However, none of the synthesized compounds shows a significant ($p < 0.05$) activity of α-Glucosidase inhibition, while acarbose indicated 73.52% inhibition at a maximum (100 μg/mL) concentration. These results indicate that the compounds **3c** and **4c** were more effective against α-Glucosidase. No reports were available about the α-Glucosidase inhibitory activities of nitro acridines and nitro phenylquinolines in literature.

Correlation study of acridine- and phenylquinoline-based derivatives

The synthesized acridines and phenylquinolines were subjected to α-Amylase and α-Glucosidase enzyme inhibition activity of Pearson correlation analysis and are given in Table 2. In α-Amylase, **3a** exhibited linear correlation with **3b** ($r = 0.95$; $p = 0.18$), **3c** ($r = 0.95$; $p = 0.18$), **4a** ($r = 0.97$; $p = 0.62$), **4b** ($r = 0.85$; $p = 0.34$), **4c** ($r = 0.93$; $p = 0.23$), and **4d** ($r = 0.88$; $p = 0.31$) and a nonlinear correlation with **3d** ($r = -0.56$; $p = 0.62$). Compound **3c** exhibited a linear correlation in all compounds except **3d** ($r = -0.77$; $p = 0.43$), and also **3c** significantly has a linear correlation with **4a** ($r = 0.99$; $p = 0.04$) and **4c** ($r = 0.99$; p = 0.04). At the same time, **3d** exhibits nonlinear correlation with all acridine- and phenylquinoline-based derivatives (Table 2).

In α-Glucosidase, **3a** exhibited linear correlation with **3c** ($r = 0.96$; $p = 0.17$), **3d** ($r = 0.62$; $p = 0.56$), **4a** ($r = 0.99$; $p = 0.06$), **4b** ($r = 0.84$; $p = 0.36$), **4c** ($r = 0.98$; $p = 0.09$), and **4d** ($r = 0.89$; $p = 0.29$) and a nonlinear correlation with **3b** ($r = -0.59$; $p = 0.59$). At the same time, **3b** exhibited a nonlinear correlation in all compounds except **3c** ($r = -0.35$; $p = 0.77$). Compound **3c** exhibits a linear correlation with remaining **3d** ($r = 0.81$; $p = 0.39$), **4a** ($r = 0.98$; $p = 0.10$), **4b** ($r = 0.95$; $p = 0.18$), **4c** ($r = 0.99$; $p = 0.07$), and **4d** ($r = 0.98$; $p = 0.11$) derivatives (Table 2). Compound **4c** exhibits the significant linear correlation with **3c** ($r = 0.99$; $p = 0.04$) and **4a** ($r = 0.99$; $p = 0.03$).

On the whole, **3c, 4a,** and **3a** demonstrated a strong linear correlation with both α-Amylase and α-Glucosidase enzyme inhibition in the majority of compounds, while **3d** demonstrates the lesser linear correlation and strong nonlinear correlation. The pharmacological investigations have demonstrated that the quinoline ring framework is available in numerous compounds showing a wide scope of biological activities [20]. The α-Amylase and α-Glucosidase enzyme inhibition activities were linearly correlated to compounds nature and its behavior.

Docking studies

Physicochemical and ADMET screening of compounds

To know about the drug-likeliness of all the synthesized compounds, their physiochemical properties were explored. Except for **3b** and **3c,** all other compounds found to obey the Lipinski's Rule of Five. In silico calculations were made to find the physicochemical properties such as TPSA (polar surface area), molecular weight, LogP (octanol-water partition coefficient), H-bond donors/acceptors, and number of rotatable bonds for all these compounds and are summarized in Table 2. The compounds with perfect ADME properties only will be approved as a drug in clinical tests, and hence, ADMET analyses of all these compounds **3a** to **4d** were predicted using Pre-ADMET software and found to exhibit satisfactory ADMET results (Table 3). All these compounds displayed very good intestinal absorption and modest permeability (except **3c**), while they subjected to in vitro study on Caco-2 cells.

The extensive plasma protein binding will increase the amount of drug that has to be absorbed before effective therapeutic levels of unbound drug are reached. The compounds **3a–4d** were studied through ADME to find their binding ability with plasma proteins; all the compounds **3a–4c** were observed to bind strongly, but the compound **4d** exhibited comparatively less binding ability. The in vitro cell permeability studies were performed using MDCK cells; all the compounds exhibited moderate performance. The CNS active drugs reported to pass across the BBB; through this study, the side effects caused by CNS inactive drugs may be avoided. In the in vivo blood-brain barrier, penetration study of compounds **3a–4d**, **3b**, and **3d** have displayed poor; **3d**, **4a**, **4b**, **4c**, and **4d** have displayed moderate; and **3a** and **3c** have displayed higher absorption to CNS.

Molecular docking study

To observe the binding mode and possible interactions of compounds with target enzymes (α-Amylase and α-Glucosidase), docking studies were performed. The 3D models of target enzymes were generated using the Swiss model server (shown in Fig. 2). The electrostatic potential surface models of enzymes (Fig. 3) reveal the distribution of charged and uncharged residues in 3D structure and which determines the binding sites for the activators/inhibitors. Molecular docking studies of compounds against active site of enzymes revealed that all of them showed atomic interactions with best docking scores dominated by hydrogen bonding with the active site residues. The most straightforward way to evaluate the performance of molecular docking is to analyze the discrepancy between the real and best-scored

Table 2 Analysis of correlation coefficients of the Pearson test which exhibit a linear correlation between the synthesized compounds α-Amylase and α-Glucosidase inhibition assays

Test samples	**3b**	**3c**	**3d**	**4a**	**4b**	**4c**	**4d**
α-Amylase							
3a	0.95	0.95	− 0.56	0.97	0.85	0.93	0.88
3b		1.00**	− 0.77	0.99*	0.96	0.99	0.70
3c			− 0.77	0.99*	0.97	0.99*	0.70
3d				− 0.72	− 0.90	− 0.82	− 0.10
4a					0.94	0.98	0.75
4b						0.98	0.51
4c							0.64
α-Glucosidase							
3a	− 0.59	0.96	0.62	0.99	0.84	0.98	0.89
3b		− 0.39	0.25	− 0.50	− 0.06	− 0.46	− 0.17
3c			0.81	0.98	0.95	0.99*	0.98
3d				0.70	0.94	0.74	0.90
4a					0.89	0.99*	0.93
4b						0.91	0.99
4c							0.95

Pearson correlation significance between the synthesized compounds considered at $*p < 0.05$ and $**p < 0.01$

conformations. The root mean square deviation (RMSD) value between the real and the best-scored conformations for docked complexes showed less than 2.0 Å. In all the docking conformations, the lengths of hydrogen bonds have shown below 5 Å. The details of docking energy (kcal/mol) and interacting residues of α-Amylase docked complexes are represented in Table 4, and the binding mode of compounds with the active site of α-Amylase has been displayed in Fig. 4. The compound **3c** found to have good docking energy (− 6.79 kcal/mol) with α-Amylase (compared with the remaining compounds) but exhibited moderate permeability in the in vitro permeability studies with Caco-2 cells (Table 4).

In all the docked conformations, the α-Amylase active site residues participated in hydrogen bonding interactions are Ser353, Asp309, Gln314, Tyr333, Glu397, Arg349, Val350, Ser352, His30, Gln56, Arg207, Asp312, Asn310, His311, Trp73, Phe307, and Glu245. The compound **3c** has not shown any hydrogen bond interactions with α-Amylase residues (Figs.

Table 3 ADMET predicted profile for compounds acquired on the webserver of Pre-ADMET

Compound	[a]% of absorption in human intestine	[b]nm/s of in vitro Caco-2 cell permeability	[c]nm/s of in vitro MDCK cell permeability	[d]% of protein binding in vitro plasma	[e]Penetration of in vivo blood-brain barrier (C. brain/C. blood)
3a	98.93	20.76	67.57	93.36	2.87
3b	98.70	21.33	74.23	93.86	0.043
3c	97.72	1.63	78.80	95.01	4.54
3d	99.12	21.54	66.05	94.15	0.085
4a	96.31	18.96	80.13	90.47	1.76
4b	96.46	23.80	87.14	90.40	1.62
4c	96.97	17.91	86.04	99.09	1.25
4d	96.41	22.08	88.12	86.45	1.92

[a] % of absorption in human intestine: 0–20% (reduced absorption); 20–70% (moderate absorption); 70–100% (superior absorption)

[b] nm/s of in vitro Caco-2 cell permeability: < 4 values are small permeability; > 4–70 values are middle permeability; and > 70 values are elevated permeability

[c] nm/s of in vitro MDCK cell permeability: < 25 are short permeability; 25–500 are core permeability; > 500 are elevated permeability

[d] % of protein binding in vitro plasma: < 90% are weak binding; > 90% are strong binding

[e] Penetration of in vivo blood brain barrier: < 0.1 (low absorption); 0.1–2.0 (middle absorption); and > 2.0 (higher absorption)

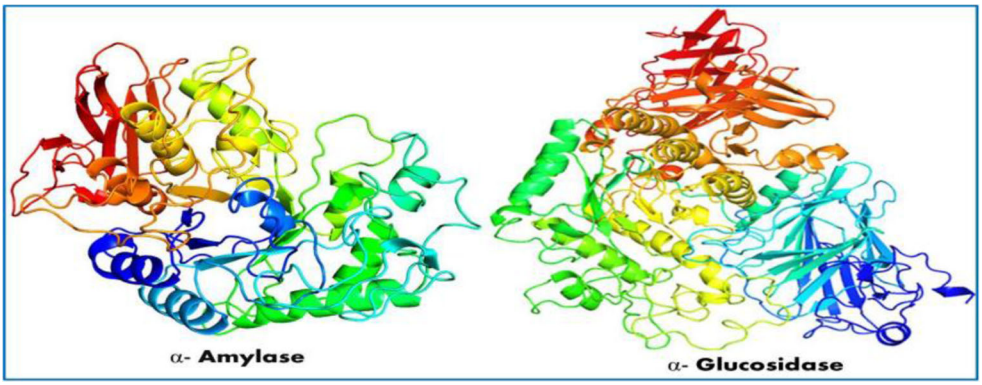

Fig. 2 3D models of α-Amylase and α-Glucosidase enzymes of rat

2 and 3c). The results of the docking analysis of α-Glucosidase revealed that compound **3c** has shown more docking energy (− 7.89 kcal/mol) compared with others (Table 5). The amino acid residues participated in hydrogen bond interactions with **3c** compound are His295, Phe297, Leu260, Gln633, Glu630, and Glu262 (Figs. 5 and 3c). The common residues such as Phe603, His295, and Leu637 were involved in polar interactions with all compounds (Fig. 5). Based on the docking results, the compound **3c** has shown the highest binding energy than the remaining compounds with both enzymes, followed by **3a** and **4c** which have shown more binding energy with amylase and glucosidase respectively. The active site residues of enzymes have participated in hydrogen bonding with all compounds examined in the present study. The interaction was disclosed that compounds may interfere/inhibit the function of enzymes in disease conditions.

Methodology

Chemistry

Melting points (m.p.) reported herein were recorded using Elchem microprocessor-based DT apparatus. ^{1}H and ^{13}CNMR spectra were recorded using Bruker 400 MHz spectrometer. High-resolution mass spectra were recorded using a Bruker MaXis HR-MS (ESI-Q-TOF-MS) instrument.

General procedure for the synthesis of compounds 3a–c and 4a–c

A mixture of compound **1** (0.1 g, 0.0005 M, 1) with either of cyclo hexan-1, 3-dione, 5, 5-dimethyl cyclohexan-1, 3-dione, cyclohexadiene, or a catalytic amount of conc. sulphuric acid was stirred in acetic acid for 12 h. After the completion of the reaction, the crude was extracted with ethyl acetate, and the organic layer was dried to obtain **3a–c**. The products **3a–c** are reduced to **4a–c** respectively by stirring with zinc dust (0.17 g, 0.0026 M) in the presence of NH_4Cl (0.16 g, 0.0026 M) in dioxane/water (1:1) for 15 min. The product was filtered and purified by column chromatography (basic alumina) using ethyl acetate/hexane (4:6) as eluent to afford the compound **4a-c**.

7-nitro-9-phenyl-3, 4-dihydroacridine-1(2*H*)-one (3a)

Yellow solid, yield 90%, m.p., 233–235 °C; IR ν/cm^{-1} = 1552 (NO_2), 1695 (C=O, ketone); ^{1}H NMR (400 MHz, $CDCl_3$), δ ppm 8.50 (dd, J = 2.8, 9.2 Hz, 1H), 8.42 (d, J =

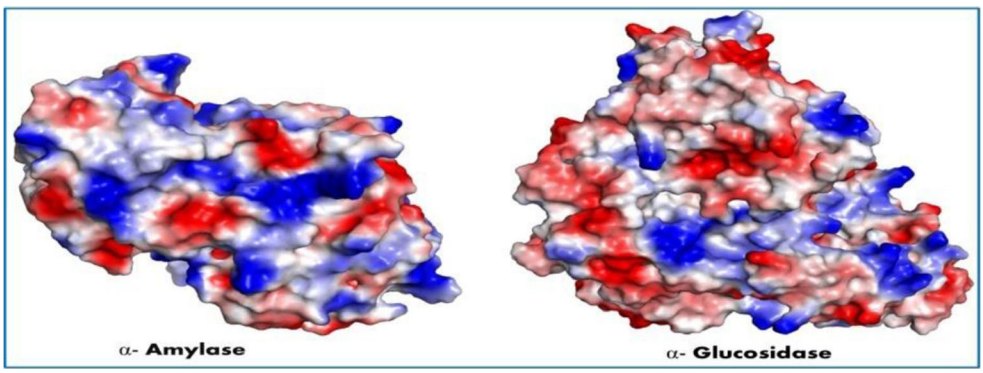

Fig. 3 The electrostatic potential surface models of α-Amylase and α-Glucosidase enzymes of the rat. Colors on the surface portrayal of the compound buildings are based on electrostatic possibilities of positive (blue) and negative (red) charged residues. The electrostatic potential of enzymes are $-45.869k_bT/e$ to $+45.869k_bT/e$ (α–Amylase) and $-61.985k_bT/e$ to $+61.985k_bT/e$ where k_b, T, and e are the Boltzmann constant, temperature, and the electron charge, respectively

Table 4 Molecular docking analysis of α-Amylase with compounds

S. No	Name of ligand	Kcal/mol of binding energy	No. of H-bonds	Contributed amino acids	Cluster of RMSD	Reference of RMSD
1	**3a**	− 7.04	8	Ser353, Asp309, Gln314, Tyr333, Glu397, Arg349	0.00	52.56
2	**3b**	− 4.39	6	His311, Asp312, Arg349, Arg207, Glu245	0.00	53.72
3	**3c**	− 7.89	-	-	0.00	64.99
4	**3d**	− 6.12	10	Val350, Ser352, His30, Gln56, Arg207, Asp312, Asn310,His311, Trp73	0.47	53.11
5	**4a**	− 5.57	4	Asp311, Arg349, Gln310, Tyr77	0.34	54.66
6	**4b**	− 4.97	3	Asp309, Arg349, Val350	0.00	55.18
7	**4c**	− 6.91	1	Val350	0.23	54.70
8	**4d**	− 6.75	6	Phe307, Asn310, Asp312, Arg207, Val350, Glu56	0.00	53.87

2.4, Hz, 1H), 8.18(d, $J = 9.2$ Hz, 1H), 7.55 (t, $J = 2.8$ Hz,3H), 7.18–7.20 (m, 2H), 3.4 (t, $J = 6.2$ Hz, 2H), 2.75 (t, $J = 6.6$ Hz, 2H), and 2.26–2.32 (m, $J = 6.5$ Hz, 2H); ^{13}CNMR (100 MHz, $CDCl_3$), δ ppm 197.1, 166.1, 153.2, 150.5, 145.6, 135.8, 130.5, 128.6, 128.1, 126.8, 125.3, 125.0, 124.9, 40.5, 34.9, and 21.0.

3, 3-dimethyl-7-nitro-9-phenyl-3, 4-dihydroacridine-1(2*H*)-one (3b)

Yellow solid, yield 92%, m.p., 230–232 °C; IR ν/cm^{-1} = 1552 (NO_2), 1693 (C=O, ketone); ^{1}H NMR (400 MHz, $CDCl_3$), δ ppm 8.50 (dd, $J = 2.8$, 9.2 Hz, 1H), 8.43 (d, $J =$ 2.4 Hz, 1H), 8.18 (d, $J = 9.2$ Hz, 1H), 7.55 (t, $J = 3.0$ Hz,3H), 7.17–7.20 (m, 2H), 3.31 (t, $J = 6.2$ Hz, 2H), 2.61 (t, $J = 6.4$ Hz, 2H), and 1.18 (s, 6H); ^{13}CNMR (100 MHz, $CDCl_3$), δ ppm 197.2, 165.1, 152.9, 150.8, 145.6, 136.8, 130.5, 128.6, 128.55, 128.1, 126.7, 125.1, 124.9, 124.2, 54.1, 48.6, 32.3, and 28.4.

5,6,7,8-tetrahydro-2-nitro-9-phenylacridine (3c)

Yellow solid, yield 85%, m.p., 226–228 °C; IR ν/cm^{-1} = 1552 (NO_2), 1695 (C=O, ketone); ^{1}H NMR (400 MHz, $CDCl_3$), δ ppm 8.35 (dd, $J = 2.4$, 9.2 Hz, 1H), 8.29 (d, $J =$ 2.4, Hz, 1H), 8.10 (d, $J = 9.2$ Hz, 1H), 7.56 (dt, $J = 7.2$, 2.8 Hz,3H), 7.24 (dd, $J = 7.8$, 1.4 Hz, 2H) 3.24 (t, $J =$ 6.6 Hz, 2H), 2.65 (t, $J = 7.0$ Hz, 2H), 2.08–1.965 (m,2H),

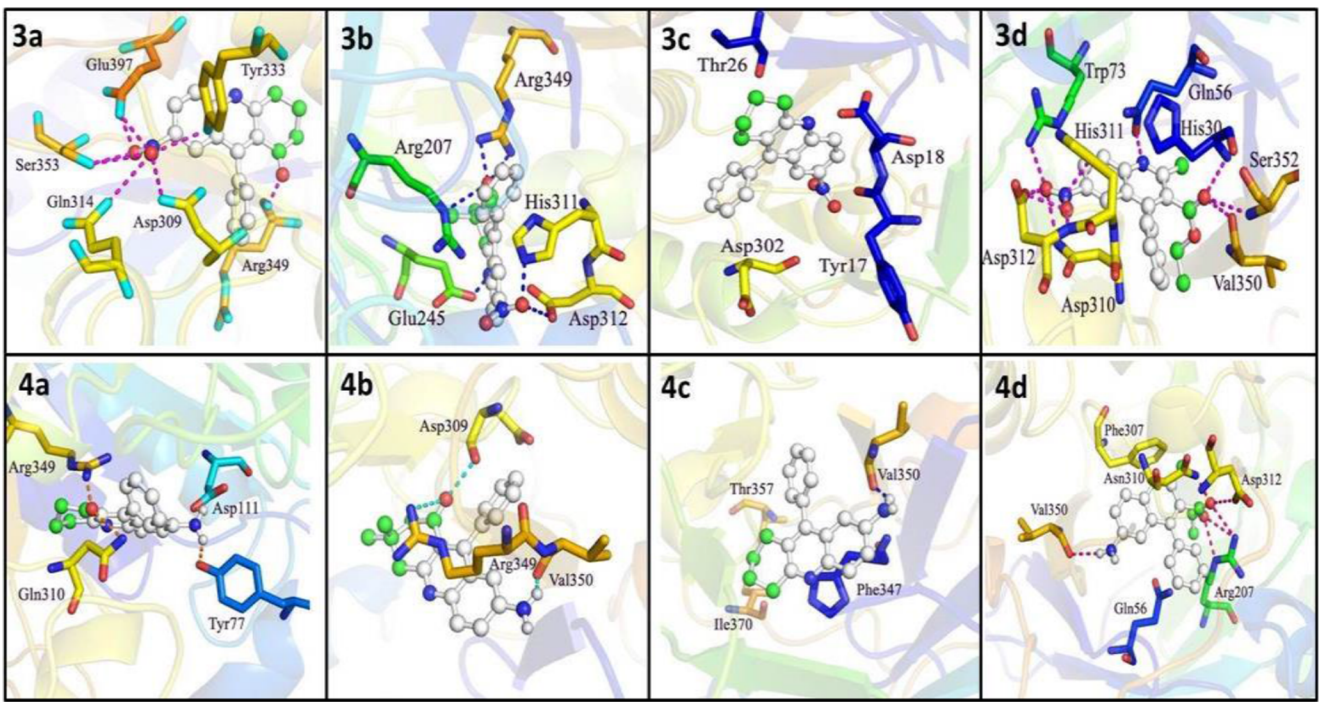

Fig. 4 Molecular interactions of compounds (**3a** to **4d**) with α-Amylase. All compounds and binding filtrates are exposed in deposits which are appeared in the ball and stick model, respectively. The dotted line represents the hydrogen bond interactions between compounds and residues

Table 5 Molecular docking analysis of α-Glucosidase with compounds

S. No	Name of ligand	Kcal/mol of binding energy	No. of H-bonds	Contributed amino acids	Cluster of RMSD	Reference of RMSD
1	**3a**	− 5.72	3	Phe603, His295, Leu637	0.00	27.25
2	**3b**	− 3.14	4	Phe603, His295, Leu637	0.09	27.39
3	**3c**	− 6.79	5	His295, Phe297, Leu260, Gln633, Glu630, Glu262	0.00	25.47
4	**3d**	− 5.61	4	Phe603, His295, Leu637	0.47	27.46
5	**4a**	− 5.37	1	Leu637	0.00	27.21
6	**4b**	− 4.65	1	Leu637	0.23	27.39
7	**4c**	− 6.47	1	Leu637	0.00	27.21
8	**4d**	− 3.83	-	-	0.00	28.13

and 1.80–1.86 (m, 2H); ^{13}C NMR (100 MHz,$CDCl_3$), δ ppm 163.6, 148.4, 148.3, 144.9, 135.4, 132.2, 131.6, 130.8, 130.1, 129.2, 129.15, 129.1, 128.94, 128.6, 125.7, 123.0, 212.9, 116.8, 34.6, 29.7, 28.1, 22.7, and 22.5.

7-amino-9-phenyl-3, 4-dihydroacridine-1(2*H*)-one (4a)

Reddish brown solid, yield 88%, m.p.:,216–218 °C; IR ν/cm^{-1} = 3446, 3305 (NH_2), 1680 (C=O, ketone); ^{1}H NMR (400 MHz, $CDCl_3$), δ ppm 7.87 (d, J = 9.2 Hz, 1H), 7.46 (m, 3H), 7.20 (dd, J = 9.2, 2.4 Hz, 1H), 7.15 (d, J = 7.6 Hz, 2H), 6.47 (d, J = 2.4 Hz, 1H), 3.85 (s, 2H), 3.30 (t, J = 6.2 Hz, 2H), 2.66 (t, J = 6.4 Hz, 2H), and 2.24–2.17 (m, 2H);^{13}C NMR (100 MHz, $CDCl_3$), δ ppm 197.4, 157.4, 147.8, 143.5, 143.0, 137.3, 128.6, 127.9, 127.1, 127.0, 126.2, 122.9, 122.8, 106.5, 39.7, 33.2, and 20.5; HRMS-ESI (m/z) calcd for $C_{19}H_{16}N_2O$ $[M]^+$ = 288.1263, found = 288.1260.

7-amino-3, 3-dimethyl-9-phenyl-3, 4-dihydroacridine-1(2*H*)-one (4b)

Yellow solid, yield 85%, m.p., 220–222 °C; IR ν/cm^{-1} = 3437, 3331 (NH_2),1680 (C=O, ketone); ^{1}H NMR (400 MHz, $CDCl_3$), δ ppm 7.81 (d, J = 9.2 Hz, 1H), 7.38–7.44 (m, 3H), 7.13 (dd, J = 9.0, 2.2 Hz, 1H), 7.08 (d, J = 6.8 Hz,2H), 6.42 (d, J = 2.0 Hz, 1H), 3.78 (bs, 2H), 3.12 (s, 2H), 2.45 (s,2H), and 1.06 (s, 6H); ^{13}C NMR (100 MHz,$CDCl_3$), δ ppm 198.4, 157.3, 148.4, 144.5, 144.3, 138.30, 129.7, 128.9, 128.2, 128.1, 127.3, 123.8, 122.9,

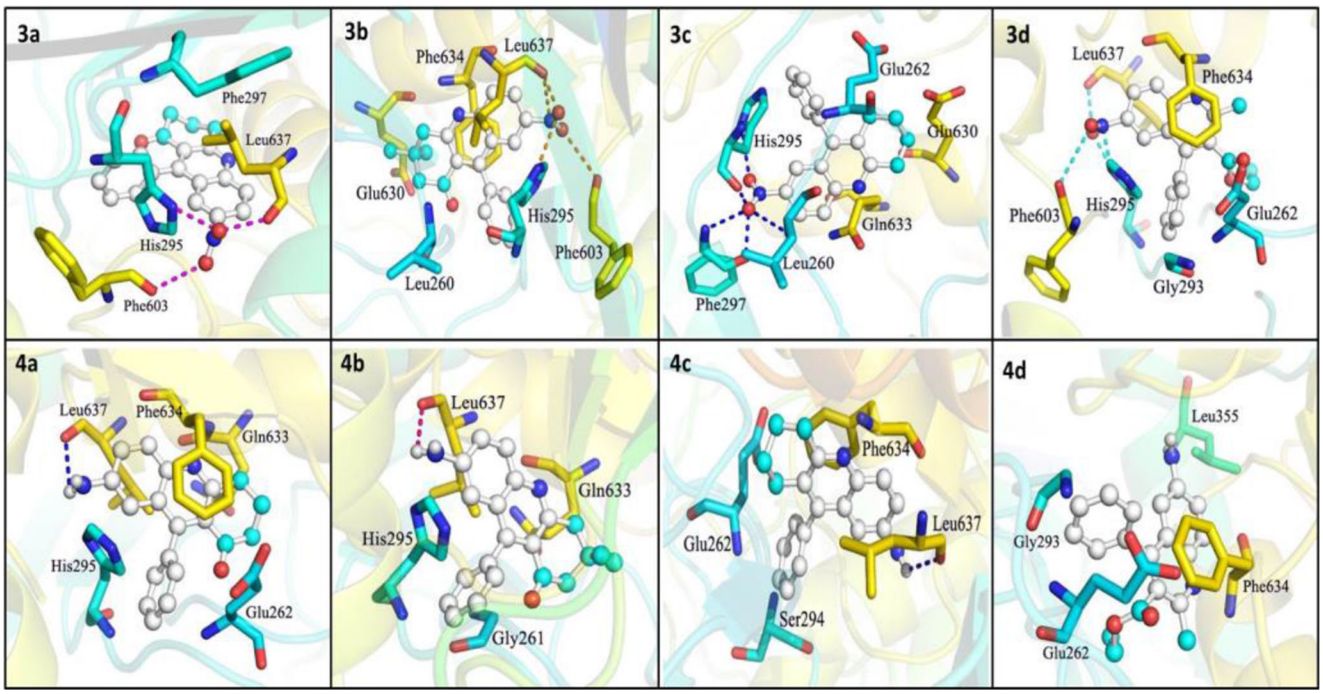

Fig. 5 The molecular interactions of compounds **3a–4d** with α-Glucosidase. All compounds and binding deposits have appeared in the ball and stick form, respectively. The dotted line represents the hydrogen bond interactions between compounds and residues

107.7, 54.3, 48.0, 32.3, and 28.4. HRMS-ESI (m/z) calcd for $C_{21}H_{20}N_2O$ $[M]^+ = 316.1576$, found = 316.1569.

9-phenyl-5, 6, 7, 8-tetrahydroacridine-2-amine (4c)

Solid compound obtained; yellow color appears, yield 80%, m.p., 218–220 °C; ^{1}H NMR (400 MHz, $CDCl_3$), δ ppm 7.83 (d, J = 8.8 Hz, 1H), 7.50 (t, J = 7.2 Hz, 2H), 7.44 (t, J = 7.4 Hz, 1H), 7.21 (t, J = 6.8 Hz,2H), 7.05 (dd J = 8.8, 2.4 Hz, 1H), 6.38 (d, J = 2.4 Hz 2H), 3.12 (t, J = 6.6 Hz, 2H), 2.53 (t, J = 6.6 Hz, 2H), 1.90–1.96 (m, 2H), and 1.72–1.78 (m, 2H); ^{13}C NMR (100 MHz,$CDCl_3$), δ ppm 155.2, 144.3, 143.6, 141.7, 137.7, 129.6, 129.2, 128.8, 128.6, 128.5, 128.1, 127.9, 127.5, 120.5, 106.2, 33.9, 28.1, 23.14, and 23.09; HRMS-ESI (m/z) calcd for $C_{19}H_{18}N_2$ $[M]^+ = 274.1470$, found = 274.1467.

General procedure for synthesis of 3d and 4d

A mixture of **1** (0.1 g, 0.0005 M, 1) with ethyl acetoacetate and a catalytic amount of ortho-phosphoric acid was stirred in ethanol for 12 h. After completion of the reaction, the crude product was poured in ice water; the obtained product **3d** was filtered, dried, and reduced by stirring with zinc dust (0.17 g, 0.0026 M) in presence of ammonium chloride (0.16 g, 0.0026 M) in dioxane/water (1:1) for 1 h. The product was filtered and purified by column chromatography (basic alumina) using ethyl acetate/hexane (4:6) as eluent.

Ethyl 2-methyl-6-nitro-4-phenylquinoline-3-carboxylate (3d)

Yellow colored solid, 95% of yielding, m.p., 210–212 °C; IR ν/cm^{-1} = 1525 (NO_2), 1724 (C=O, ketone); ^{1}H NMR (400 MHz, $CDCl_3$), δ ppm 8.56 (d, J = 2.4 Hz, 1H), 8.50 (dd, J = 9.2, 2.4 Hz, 1H), 8.22 (d, J = 9.2 Hz, 1H), 7.57 (t, J = 3.20 Hz, 3H), 7.39 (dd, J = 6.0, 2.4 Hz, 2H), 4.12 (q, J = 7.20 Hz, 2H), 2.85 (s, 3H), and 0.99 (t, J = 7.0, 3H); ^{13}C NMR (100 MHz, $CDCl_3$), δ ppm 167.5, 158.9, 149.70, 148.0,145.6, 134.1, 130.8, 129.4, 129.3, 129.2, 128.8, 124.5, 123.8, 123.52, 61.80, 24.15, and 13.64.

Ethyl 6-amino-2-methyl-4-phenylquinoline-3-carboxylate (4d)

Yellow solid, yield 90%, m.p., 206–208 °C; IR ν/cm^{-1} = 3462, 3352 (NH_2); 1716 (C=O, ketone); ^{1}H NMR (400 MHz, $CDCl_3$): δ ppm 7.80 (d, J = 8.8 Hz, 1H), 7.37 (m, 3H), 7.26 (d, J = 6.6 Hz, 2H), 7.06 (d, J = 8.0 Hz, 1H), 6.54 (s, 1H), 4.12 (q, J = 7.20 Hz, 2H), 3.79 (s, 2H), 2.63 (s, 3H), and 0.86 (t, J = 7.20 Hz, 3H); ^{13}CNMR (100 MHz, $CDCl_3$): δ ppm 168.83, 150.50, 144.64, 143.96, 142.81, 136.27, 129.96, 129.38, 128.21, 127.57, 126.55, 122.12, 106.48, 61.21, 23.30, and 13.65. HRMS-ESI (m/z) calcd for $C_{19}H_{18}N_2O_2$ $[M]^+ = 306.1368$, found = 306.1365.

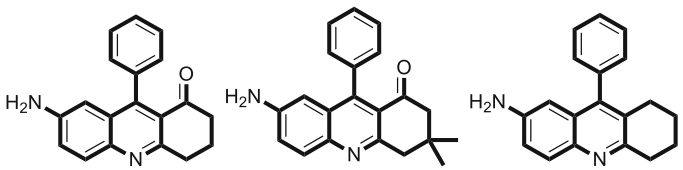

Biological activity

α-Amylase inhibition assay

The α-Amylase enzyme inhibition activity was carried out by the standard reference method [21]. In a test tube, 1 mL of 1% phosphate buffer prepared in starch solution was incubated with an α-Amylase enzyme (500 μL) for 10 min at room temperature. About 1 mL of various concentrations (20–100 μg/mL) of acridine (**3a−c**; **4a−c**) and phenylquinoline (**3d**, **4d**) derivatives were added to the above-incubated enzyme solution; after that 1 mL of NaOH (2 M) solution was added to freeze the reaction. Then 1 mL of 3, 5-dinitro salicylic acid (DNS) was added and maintained in a water bath for 5 min. The contents of the test tube were cooled in water, the final volume was made up to 10 mL using distilled water, and the absorbance was measured at 540 nm against blank (without test sample) in UV-Vis spectrophotometer. Acarbose was used as a reference drug.

Determination of α-Glucosidase inhibition assay

The α-Glucosidase enzyme inhibitory activity was determined by a slightly modified method [22]. A 1 mg of *Saccharomyces cerevisiae* isolated α-Glucosidase enzyme was dissolved in 100 mL of phosphate buffer saline (pH 6.8) containing 200 mg of bovine serum albumin. The acridine and phenylquinoline derivatives were prepared in 20–100 μg/mL concentration. From that 10 μL of the test solution was taken and premixed with 490 μL phosphate buffer (pH 6.8) and 250 μL of p-nitro-phenyl-α-d-glucopyranoside (*p-NPG)*

(5 mM). After 5 min. of pre-incubation at 37 °C, 250 μL of α-Glucosidase (0.15 unit/mL) was added and incubated at 37 °C for further 15 min. To quench the reaction, 2 mL sodium carbonate (200 mM) was added. The activity of the α-Glucosidase enzyme was observed at 405 nm using UV-Vis spectrophotometer by measuring the quantity of *p*-nitrophenol released from *p*-NPG. Acarbose was used as a standard.

The following equation was utilized to measuring the percentage of both investigated enzymes inhibition,

$$\% \text{ inhibition of enzyme} = [\text{Abs}_{\text{Control}} - \text{Abs}_{\text{Tested compound}}] / [\text{Abs}_{\text{Control}}] \times 100$$

whereas Abs = Absorbance.

Docking studies

Prediction of drug-likeness and ADMET screening of compounds

For a drug candidate to be sufficiently bio-available and ultimately be a commercial success, its pharmacodynamic activity needs to be in consistent with its structure and physicochemical and biological properties [23–25]. In order to check the drug-likeness, affinity, and selectivity of lead molecules, there is necessary to maintain the molecular weight and lipophilicity. Lipinski's Rule of Five was used to predict the in silico physicochemical properties of all compounds [26] using the Molinspiration software. Bioavailability involves the intestinal absorption and distribution, which are determined by the stability, dissolution, solubility, permeability, dosage, first-pass metabolism, and various mechanisms of action of drug molecule [27].

Molecular docking studies

Homology models of α-Amylase and α-Glucosidase were generated using Swiss model program according to the Cheemanapalli et al. (2016) method [28]. The FASTA sequences of pancreatic alpha amylase (Gen Bank ID: AAA40725.2) and glucosidase (Gen Bank ID: AAH61753.1) of *Rattus norvegicus* were obtained from NCBI. To make a three dimensional protein models, the Swiss model program uses template structures of human enzyme models such as 1B2Y (α-Amylase) and 5KZW (α-Glucosidase) respectively.

Statistical data analysis

The obtained data was performed by one way ANOVA followed by Duncan Post Hoc using SPSS 16.0 package. $p < 0.05$ values were considered significant. All qualities were communicated as mean ± SD for triplicate. Graph Pad Prism 5.1 (Graph cushion programming, Inc., La Jolla, CA, USA) was used to determine the IC_{50} values.

Conclusion

In the present work, we have productively achieved our objective designate derivatives of **4a–d.** All the compounds were established by appropriate experimental and spectroscopic techniques. Synthesized derivatives (**3a–d** and **4a–d**) were evaluated for in vitro α-Amylase and α-Glucosidase inhibitory activities. Among the tested derivatives, 7-nitro-9-phenyl-1, 2, 4, 4-tetrahydroacridine (**3c**) compound showed good inhibitory activity for α-Amylase and α-Glucosidase with the IC_{50} values of 200.61 ± 9.71 μmol/mL and 197.76 ± 8.22 μmol/mL, respectively, and 9-phenyl-5, 6, 7, 8-tetrahydroacridine-2-amine (304.28 ± 3.51 μmol/mL and 278.86 ± 3.24 μmol/mL), and 7-nitro-9-phenyl-3, 4-dihydroacridine-1(2*H*)-one (243.78 ± 13.25 μmol/mL and 296.57 ± 10.66 μmol/mL) show moderate inhibitory activity against α-Amylase and α-Glucosidase. The in silico molecular docking studies are in good conformity with the in vitro antidiabetic studies. The molecular docking calculations showed that hydrogen bonds interactions and desolation energies play a key role in binding. These features are well thought out for scheming new inhibitors for α-Amylase and α-Glucosidase enzymes.

Acknowledgments The authors are grateful to the VIT University in Vellore, India, for giving facilities to convey explore work. The authors are likewise appreciative to the Department of Biotechnology, School of Herbal Studies, and Nature Sciences in Dravidian University, Kuppam, India.

Compliance with ethical standards

Conflict of interest The authors declare that they have no conflict of interest

References

1. Palanuvej C, Hokputsa S, Tunsaringkarn T, Ruangrungsi N (2009). Sci Pharm 77(4):837
2. Chang LS, Li CB, Qin N, Jin MN, Duan HQ (2012). Chem Biodivers 9(1):162
3. Ditzel J, Lervang HH (2009). Diabetes, Metabolic Syndrome and Obesity: Targets and Therapy 2:173
4. Sales PM, Souza PM, Simeoni LA, Magalhães PO, Silveira D, Pharm J (2012). Pharm Sci 15:141–183
5. Lebovitz HE (1998). Diabetes Rev 6:132–145
6. Tundis R, Loizzo MR, Menichini F (2010). Med Chem 10:315–331
7. Sondhi SM, Singh J, Rani R, Gupta PP, Agrawal SK, Saxena AK (2010). Eur J Med Chem 45:555–563

8. Gupta SK (2004). Drug screening methods (Pre clinical evaluation of new drugs) 2nd edn. Jaypee Medical Publishers (P) Ltd, New Delhi, pp 306–309
9. Korth C, May BC, Cohen FE, Prusiner SB (2001). Proc Natl Acad Sci U S A 98:9836–9841
10. Temple MD, McFadyen WD, Holmes RJ, Denny WA, Murray V (2000). Biochemistry. 39:5593–5599
11. Riera X, Moreno V, Noe V, Font-Bardía M, Solans X (2007). Bioinorg Chem Appl:98732 https://doi.org/10.1155/2007/98732
12. Jiang D, Tam AB, Alagappan M, Hay MP, Gupta A, Kozak MM, Le QT (2016). Mol Cancer Them 15:2055–2065
13. Cholewiński G, Dzierzbicka K, Kołodziejczyk AM (2011). Pharmacol Rep 63:305–336
14. Pang X, Chen C, Su X, Li M, Wen L (2014). Org Lett 16:6228–6231
15. Peacocke AR, Nicholson BH, Dean ACR, Clayson DB, Henry DW (1973) Heterocycl. Compd. John Wiley, New York, p 723
16. Ketron AC, Denny WA, Graves DE, Osheroff N (2012). Biochemistry. 51:1730–1739
17. Amuthalakshmi S, Smith AA (2013). Adv Biol Res 7:248–252
18. Kubinyi H (1998). Curr Opin Drug Discov Devel 1:16–27
19. Levetan C (2007). Curr Med Res Opin 23:945–952
20. Rajesh YB (2018). Quinoline Heterocycles: synthesis and bioactivity In heterocycles-synthesis and biological activities. Intechopen.com. https://doi.org/10.5772/intechopen.81239
21. Hansawasdi C, Kawabata J, Kasai T (2000). Biosci Biotechnol Biochem 64:1041–1043
22. Kim YM, Jeong YK, Wang MH, Lee WY, Rhee HI (2005). Nutrition. 21:756–761
23. Li AP (2001). Drug Discov Today 6:357–366
24. Lipinski CA (2000). J Pharmacol Toxicol Methods 44:235–249
25. Sugiyama Y (2005). Drug Discov Today 10:1577–1579
26. Lipinski CA, Lombardo F, Dominy BW, Feeney PJ (2012). Adv Drug Deliv Rev 64:4–17
27. Agoram B, Woltosz WS, Bolger MB (2001). Adv Drug Deliv Rev 50:S41–S67
28. Cheemanapalli S, Anuradha CM, Madhusudhana P, Mahesh M, Raghavendra PB, Kumar CS (2016). Anti Cancer Agents Med Chem 16:1496–1510